Investigation of the Elastic Properties of Poly (methyl methacrylate) Reinforced with Graphene Nanoplatelets

M. MUHAMMETTURSUN[1], T. BEL[1], E. KOCACINAR[1], E. ERMAN[1], F.B. GUL[1], A. T. AUGOUSTI[2], N. BAYDOGAN[1*]

[1]Istanbul Technical University, Energy Institute, Ayazaga Campus, Maslak, 34469, Istanbul, Turkey

[2]Faculty of Science, Engineering and Computing, Kingston University, London, SW15 3DW, UK

Abstract

The technique for synthesis of poly (methyl methacrylate) by atom transfer radical polymerization has been strengthened by using graphene nanoplatelets to enhance the elastic properties of the polymer. In order to improve practical, economical and mechanical performance, the requirements for effective implementation of production control as a smart bulk polymer nanocomposite were determined for cost-effective bulk production. Three-dimensional inspection (using an ultrasound interrogation method for the whole volume under test) confirmed the synthesis of the nanocomposite to be free of agglomeration and bubbles. As a result of this elimination of defects, an enhancement in compressive strength of 42.7% was achieved and the Rockwell hardness was increased by 19.9 % through the addition of graphene nanoplatelets at 2 wt% by mass. The deformation and mechanical failure properties have been characterised in the mechanical enhancement of the the polymer nanocomposite. Elastic parameters determined using ultrasound testing identified that changes in the structural features following the addition of these GNPs were uniquely connected to the enhancements in these elastic parameters (such as Young's modulus, Poisson's ratio, shear modulus and microhardness) of the poly (methyl methacrylate) / graphene nanoplatelets nanocomposite.

***Corresponding Author:** Nilgun BAYDOGAN, dogannil@itu.edu.tr, +902122853492 (tel.),

1. Introduction

Poly (methyl methacrylate) (PMMA) is a clear and transparent thermoplastic and a lightweight material with multi-scale functional applications for medical sensors, solar cells, electronics and aerospace technologies [1-4]. Users in the research or industrial application areas have sought to make demanding modifications in the elastic parameters of PMMA by

using polymer nanofillers to produce high quality at low prices [1-2]. However, the mechanical properties of PMMA are poor for high-tech applications [5]. The relative weakness of PMMA under fatigue rupture presents a major problem for its longer-term use in service applications [6].

Nanocomposite materials can improve this poor mechanical performance of the polymer. The nanoparticles can be used as fillers to improve the structural characteristics of the polymer [7]. Graphene nanoplatelets (GNPs) provide a lower mass density, superior mechanical properties as GNPs contain monolayer graphene exhibiting these excellent properties. The production of other carbon-based nanofillers (such as carbon nanotubes-CNTs and carbon nanofibers-CF) usually require expensive and complex equipment and higher energy consumption (utilising techniques such as chemical vapor decomposition, arc discharge, laser ablation, etc.). However, high-quality GNPs can be derived from abundant natural graphite via relatively convenient methods. This makes GNPs a cost-effective nanofiller to use as a nanocomposite in many application areas [8]. GNP clustering results in several difficulties at higher GNP concentrations with the consequent deterioration in the mechanical properties of the polymer nanocomposite [9]. The rise in the number of defects with GNP clustering causes problems as such defects can serve as the starting points for cracks in the nanocomposite [10-12]. The enhancement of the elastic properties of the nanocomposite (as a lightweight material) means that it can provide protection for equipment from mechanical damage in longer-term service. Systems payloads can be decreased considerably through the development of such a modified lightweight polymer. Protection of equipment against mechanical damage is of potential interest and significance for telecommunication systems including lightweight nanocomposites for space applications [11-12]. The atom transfer radical polymerization (ATRP) technique provides an opportunity to prepare novel multifunctional materials with good control of the polymer's molecular weight, polydispersity index and end-group functionality through the addition of graphene nanoparticles [13-18]. For instance, the use of graphene has improved the physical properties of PMMA as a reinforcing agent for bone cement [16]. The ATRP functional groups are more suitable than ionic polymerization as a tuning method for industrial applications as the cross-linkable PMMA can be synthesized in a controlled manner by using MMA monomers in the ATRP method [12]. The improvement in the mechanical properties with the addition of GNP at 2 wt.% indicated that the influence of crosslink density on the modification of elastic properties of the nanocomposite reached an optimum level at of 2 wt% GNP. The use of traditional polymer composites is restricted by their bulkiness, high rigidity, and difficulty in processing. The forces applied can produce

compressive stresses whose magnitude is difficult to determine in practice. The utilization of newer bulk polymers is better at distributing these forces (due to the torque transmitted by the bonded polymer composite parts). The development of nanocomposites by the addition of nanoparticles modifies the mechanical properties of nanocomposites and will likely drive its medical use via the Internet of Nano Things (IoNT) systems in the near future [17], in particular by the modification of the elastic properties. Inspection of the effect of GNPs in improving the elastic mechanical properties of PMMA using ultrasound techniques has not been widely reported previously in the literature. The ATRP method (including the surface-initiated controlled radical polymerization technique) has been used here in conjunction with ultrasound monitoring to determine the optimum bulk material size needed to produce a satisfactory mechanical improvement with low density and optimum thickness.

The polymer nanocomposites with suitable mechanical performance are only obtained up to ~ 0.5 wt.% nanoparticle addition in literature and this is a relatively minor amount [9-12]. In this study, the synthes of a PMMA/GNPS nanocomposite with a suitable mechanical performance with a GNP content of 2 wt.% supports the development of next-generation nanocomposite systems. The modulus values rise as GNP concentration increases. When the GNP concentration is greater than >2%, this influences its mechanical properties. It is suggested that the nanoparticle distribution is very important for the development of the mechanical changes in this study. If it was more than 2%, the polymer nanocomposite does not have an appropriate homogeneous structure. Deterioration of the homogeneity of the structure started to affect adversely the improvement in the mechanical performance of the polymer nanocomposite. The modified nanocomposite demonstrated the enhancement of its capability of the elastic parameters (such as the increase of the shear modulus, Young's modulus and the microhardness). The increase of Young module's (stress/strain) indicated a stiffer structure with the enhancement of the nanocomposite density as a result of the increase in GNP content. Hence, the improvement of the stiffness with the enhancement of the mechanical functions will help to prolong the service life of products in markets. The stress was distributed along the length of the nanocomposite supporting the development of valuable products derived from the nanocomposite in this study. Hence, the optimum weight distribution providing protection of the centre of mass will help to ensure the optimum weight reduction providing wear reduction at the contact points. The modified PMMA/GNPs nanocomposite has proved to be a good candidate in resisting mechanical damage (such as shearing and compressive stresses) in this study. Technological modifications in this study have provided comprehensive and in-depth experimental investigations of the enhancement of

the elastic properties. The strengthening of this nanocomposite has helped to improvethe engineering capabilities of PMMA by the addition of GNPs. The modification of this nanocomposite has helped to provide a deeper exploration of the elastic features of this polymer nanocomposite for various applications. The use of this modified nanocomposite will open up new demands for advanced substrate applications in industrial areas including medical sensors, solar cells, electronics and aerospace technologies.

2. Experimental

In situ ATRP polymerization was used as the dispersion method. The schematic diagram displaying the steps in the polymerization process used to make the PMMA/GNPs nanocomposite is presented in Figure 1. Copper (I) bromide (CuBr) was chosen as the catalyst for further optimization. The use of a catalyst here provided several advantages such as higher synthetic efficiency, lower cost and a simpler process. The main advantages of this reaction were the use of readily available starting materials and optimal product yields.

2.1.Synthesis of Poly (methyl methacrylate) Reinforced with Graphene Nanoplatelets

The GNPs used in this study was purchased from Merck 99.5+ % purified, with a thickness of 6 nm, a surface area of 150 m^2/g, and a surface diameter of 5 μm. The preparation and measurements were carried out inside an AtmosBag (Sigma-Aldrich) in argon to achieve practical and cost-effective polymer nanocomposite production conditions. Bu_4NBr (1.211 g) was used as the solvent and CuBr (0.067 g, 0.47 mmol) was utilized as the catalyst. GNPs were added to tubes (8 × 2.5 cm) at four different concentrations (0.25, 0.5, 1, 2 wt.% in AtmosBag. EBIB (at 00.092 g) was used as an initiator so that it provided temperature control of the polymerization process as well as cost benefits. A regulator was used in the experiments and extra pure argon has been used during the synthesis. When the measurements were finished, the tubes were sealed with a rubber seal and taken out of the AtmosBag. Methyl Methacrylate (MMA) (28.2 g, 0.282 mol) was used as the monomer and it was added into the tube. Pentamethyldiethylenetriamine (PMDETA) was added at 0.081 g, 0.47mmol, being an inexpensive ATRP ligand. The tubes were put on a rotating shaker to avoid cracking of the GNP in the polymer solution. The solution was mixed for 15 min. and the mixture was degassed through a glass frit with pure argon for 60 min for the removal of dissolved gases from solution and to eliminate bubbling. The tube was sealed once more with a rubber seal followed by parafilm. The mixture was taken out of the AtmosBag and the tubes placed in a silicon oil bath on a rotating shaker. The mixture was maintained at 60°C vacuum for 12 h. The samples were prepared by casting in molds. Then the mixture was placed in a vacuum at room temperature for 30 min to remove entrapped air.

2.2 Structural Characterization Methods

Fourier Transform Infrared (FTIR) Spectroscopy provided some information about chemical bonds and the relevant chemical functional groups [19]. The infrared spectrum in this study indicated the absorption peaks that are a "fingerprint" of PMMA/GNPs nanocomposites. The FTIR measurements were carried out using a Bruker ALPHA spectrometer. XRD analysis was carried out to investigate the structural characterization by using a PANALYTICAL diffractometer with Cu K_α radiation (λ = 1.541 Å) with a scanning speed of 2°/min (operating at 40 kV and 40 mA).

2.3. Mechanical Tests

Rockwell hardness (M scale) was measured by a Zwick Roell ZHR hardness tester using a steel ball 6.35 mm in diameter and a load of 100 kg. Compression tests were conducted using a Shimadzu Ag-Ic 100 KN universal testing machine. The crosshead speed of the machine was 3 mm/min. The sample height was 4 cm, and the diameter was 2 cm for each sample.

2.4. Elastic Properties of PMMA/GNPs Nanocomposite

Ultrasonic testing was applied to check nondestructively for imperfections in the PMMA/GNPs nanocomposite. The reflections obtained helped to eliminate volumetric defects in PMMA/GNPs nanocomposite These reflections from bulk tests of the pure PMMA were compared with the results of PMMA/GNPs nanocomposite (at different levels of GNP content). The results of PMMA/GNPs nanocomposite (at 2 wt. % GNPs amount) for Rockwell hardness showed an increase of 19.9 %. In addition, the compressive strength rose by 42.7 %. The improvement in physical properties is attributed to the control of production parameters of the advanced nanocomposite by the use of the ATRP method in this study compared to other methods in the literature. Efficient interfacial interactions between GNPs and PMMA can influence significantly the mechanical properties of the nanocomposite at low concentrations of GNPs. The speed of sound in the polymer nanocomposite was determined using the ultrasonic test technique in order to calculate Poisson's ratio, the Shear modulus, Young's modulus, and the microhardness of the bulk material according to techniques described in the literature [20-21]. Sound waves propagate as both longitudinal and transverse (or shear) waves in solids, as these can support both axial and transverse stresses. The speeds of longitudinal and shear waves respectively are given by Eq. 1- 2 [22]:

$$C_L = \sqrt{\frac{E(1-\nu)}{\rho(1+\nu)(1-2\nu)}} \quad (1)$$

$$C_T = \sqrt{\frac{E}{2\rho(1+\nu)}} = \sqrt{\frac{G}{\rho}} \quad (2)$$

where [23]:

ρ: density of the solid material.

E: Young's modulus (or elastic modulus), which is the ratio of stress to longitudinal strain within the elastic limit.

ν: Poisson's ratio, which is the ratio of lateral strain to longitudinal strain when the solid material is elastically stretched.

G: shear modulus, which is the ratio of the tangential force per unit area to angular deformation produced in the body.

Solving these equations for E and ν gives

H: Microhardness, which is defined as the ratio of the load applied by the indenter (kg) to the unrecovered projected area A (mm^2) [24].

As ρ, C_L and C_T were determined by measurement then ν, E, G and H are given by Eqs.3-6.

$$\nu = \frac{1-2\left(\frac{C_T}{C_L}\right)^2}{2-2\left(\frac{C_T}{C_L}\right)^2} \quad (3)$$

$$E = 2\rho C_T^2(1+\nu) \quad (4)$$

$$G = \rho C_T^2 \quad (5)$$

$$H = \frac{[(1-2\nu)E]}{[6(1+\nu)]} \quad (6)$$

During ultrasonic testing, the ultrasound transducer produces a pulse at the surface of the solid material, which travels through the material and an echo reflects wherever there is a change in the acoustic impedance of the material, as occurs when it meets a crack, for example. An ultrasound transducer receives these echoes, including a final one as the ultrasound pulse reflects from the opposite face of the material, attenuating over distance [6].

The speed of the longitudinal and transverse waves in the solid can be obtained from the measured round-trip transit time, Δt, and the measured thickness (d) of material via Eq.7.

$$c = \frac{2d}{\Delta t} \tag{7}$$

It is thus possible to obtain Poisson's ratio, Young's modulus, the shear modulus and the microhardness of the solid material in the bulk [20].

3. Results and Discussions

The improvement of the interface between the GNPs and the nanocomposite is of importance [25]. The results of FTIR analysis for both pure PMMA and GNPs/PMMA nanocomposite samples are presented in Figure 2. The main absorption peaks for pure PMMA and GNPs/PMMA nanocomposite are visible at 2992 cm^{-1} ($O–CH_3$, C–H stretching), 2948 cm^{-1} ($C–CH_3$, C–H stretching), 1729 cm^{-1} (C=O stretching), 1434 cm^{-1} ($O–CH_3$ bending), 1382 cm^{-1} ($C–CH_3$ bending), 1238 cm^{-1} (C–C–O stretching), 1189 cm^{-1} (C–O–C bending), 1145 cm^{-1} (CH_2 bending) and 753 cm^{-1} (C=O bending) [26-28]. There is not much research available concerning the effect of bonding interaction between the PMMA and GNPs on the FTIR spectrum of the composite. The PMMA/GNPs nanocomposites fabricated here presented similar absorption peaks as a result of the variations in the bonding interaction between PMMA and GNPs at different concentrations of the GNPs. Interaction between the GNPs nanofiller and the PMMA polymer matrix indicated slight changes in the PMMA/GNPs nanocomposite FTIR spectrum when the GNP reached 2 wt % according to the FTIR results. The slight decrease in the intensity of the peaks at 2 wt% GNP indicated a progressive reduction in the transmitted intensity at the frequencies highlighted in Figure 2. However, there was no shift in the peak positions at any of the doping concentrations which indicates that the electron distribution in the molecular bonds has not changed.

A structural characterization of the nanocomposite was carried out using XRD analysis to examine the effect of the GNPs nanofiller on PMMA. The XRD diffraction patterns of the nanocomposite displayed characteristic peaks at ~26.5° corresponding to the stacking of the graphene monolayers at a separation of 0.34 nm [29]. XRD diffraction patterns for PMMA, GNPs and a range of PMMA/GNPs nanocomposite samples are presented in Figure 3. A strong sharp diffraction peak around ~ 26.5° represents the GNPs (002) diffraction plane. Additional smaller peaks in the GNPs spectrum may be distinguished at ~44° (100) and at ~54° (004). Pure PMMA produced using the ATRP method was determined to have a small

narrow peak at ~23° in this study, which is attribable to the non-exchanged salt-containing Br– ions according to the literature [30]. The increased intensity of the diffraction planes at higher concentrations of GNPs is attributed to the larger number of stacked graphene layers [31-38]. The peak at ~23° was attributed to the non-exchanged salt-containing CuBr and solvent Bu4NBr in PMMA, and it remained clearly visible at all GNPs concentrations. However, the GNPs peak was not clearly distinguishable at the lower sample concentrations. The characteristic peak of GNPs at ~26.5° is barely distinguishable at 0.5 wt. % GNPs concentration. The increase in the diffraction peak intensity due to the (002) diffraction plane indicated an increased crystallinity in the 1 wt. % GNPs sample. Thus we infer that the increased concentration of GNPs causes a slight increase in the crystallinity of the nanocomposite samples, which may therefore affect their mechanical properties, and this is investigated further below.

The elastic properties for pure PMMA have been determined by Afifi et al. [39]. The increase in hardness in PMMA/GNPs nanocomposites was investigated by Das et al. and Al-Saadi et al. [40-41]. Strong interfacial adhesion between the GNPs and the polymer matrix is crucial for effective reinforcement [42]. Changes in Poisson's ratio (ν), shear modulus (G), Young's modulus (E) and microhardness (H) were calculated based on the measured values of density and the speed of ultrasonic waves determined using ultrasonic techniques, and the results are presented in Table 1. The elastic properties are increased slightly with the increase in the GNPs concentration according to our measurements. The shear modulus increased by 19.5%; Young's modulus increased by 16.8 %, and the microhardness of the PMMA matrix increased by 14.2% with the addition of GNPs at a concentration of 2 wt.%. The ultrasonic signal obtained using non-destructive testing (NDT) indicated no reflections from the interior of the material, thereby showing that the synthesis technique at these levels of GNPs concentration was reliable in producing a bulk material without obvious defects. The use of ultrasound velocity testing to determine the polymer samples elastic properties had some advantages (foregoing the need for DMA test results). The main advantage of the ultrasound test was that it was based on wave propagation principles. Therefore, only small sensors were required to provide sensitive information on the elastic state of the polymer samples. The density of the samples introduced some variations in their elastic properties.

The application of ultrasound testing did not require a separate experiment and was evaluated directly and practically from the values of the acoustic wavelength. The main advantage of using the ultrasound technique (over DMA analysis) was that the ultrasound parameters were evaluated at the same time, saving considerable time in analysis, especially where some data

needed to be evaluated separately. The versatility of the ultrasound technique has significant advantages as it was applied to the polymer directly in the polymer moulding. Hence, the requirements for effective implementation of production control as a smart bulk polymer nanocomposite were determined for cost-effective bulk production along with the improvement in the practical, economical and mechanical performance.

The Rockwell hardness value indicated an increase in hardness with the increase of GNPs concentration as depicted in Figure 4. The hardness of pure PMMA increased from 85 to 101 HRM with the addition of 2 wt.% GNPs, corresponding to an increase of nearly 20 %. Both the concentration level and the associated large surface area of GNPs are important for the structural improvement in these nanocomposites [2, 33]. There is an interfacial interaction between the GNPs and the PMMA [43]. The enhancement in compressive strength at low concentration of GNPs indicated the helpful effect of GNPs concentration in raising the compressive strength. Images of the PMMA/GNPs nanocomposite at the end of the compression test indicate the extent and nature of the damage (Figure 5a). The surface morphology of the nanocomposite with a maximal concentration of GNPs (2 wt.%) was investigated to evaluate the surface properties using an SEM (Figure 5b). The structural characterization results show that the use of GNPs supports the ideal of obtaining crack-free advanced polymer nanocomposites for load-bearing component applications, thereby offering significant potential in advanced lightweight material applications.

The addition of GNPs into the PMMA increased the compressive strength of the PMMA (Figure 6). The compressive strength of PMMA was improved from 90.2 to 127.7 MPa as the GNPs concentration increased. The compressive strength reached a maximum value at 2 wt.% and its value increased by 42.7% with respect to pure PMMA. It is presumed that the stress has been significantly transferred from the PMMA matrix to the GNPs. Hence it has been possible to obtain a substantial improvement in the mechanical properties of the polymeric matrix. Changes to the elastic properties of PMMA/GNPs nanocomposite are summarized (in Table 1. A degradation in the mechanical performance can result from cracks (or pores) and GNPs clustering in the PMMA [13-15]. The mechanical test results (Figure 4 and Figure 6) have evidenced the improvement in the mechanical performance of the polymer nanocomposite via the addition of GNPs. Some cracks were visible in the samples of PMMA and PMMA/GNPs (at 0.25 wt%) according to the compression test results (Figure 6), but the presence of these cracks decreased in the PMMA/0.5%-2% GNPs samples. This improvement in hardness (Figure 4) was supported by the improvement shown by the compression test

results (Figure 6) when the GNPs concentration increased to 2 wt% GNPs. Raman spectroscopy can be used as an excellent tool to structurally characterize carbon materials and it can indicate changes in the GNPs concentration (deduced from at ~1350, ~2900 and ~ 1580 cm−1) [44]. The peak intensities of GNPs gradually diminish with the increased number of graphene layers in the previous studies [45]. Raman analysis results have demonstrated three main peak changes in Figure 7 dependent on the GNP concentration (~1350, ~2700 and ~ 1580 cm−1) in this study. The intensities of the Raman peaks decreased slightly for all peaks as a result of the increase in the number of graphene layers. Moreover, FTIR analysis results (Figure 2) have exhibited a similar slight peak intensity decrease with the rise in GNP concentration in this study.

It is proposed that the use of the synthesis process results in an optimal interaction between the GNPs and the PMMA matrix in this study. It was possible to avoid agglomeration, cracks and pores in the nanocomposite structure based on control of the production parameters in this study, such as the quantity of the chemicals used, synthesis time and the use of a neutral argon atmosphere during production. GNPs at a concentration of 2 wt. % have emerged as a promising nanofiller for PMMA based nanocomposites due to their remarkable mechanical properties, and optimal production parameters have been established by the application of NDT. It is noted that the physical performance relates to the structural characteristics of PMMA and its performance can be changed with the formation of PMMA/Colemanite composite [46-57]. Investigations of the matrix base PMMA used in this research have been carried out in space research at the International Space Station (ISS) [53-55]. There is a relationship between the molecular weight and the mechanical properties of polymers – in general increasing the molecular weight improves of the mechanical properties of the polymers [54]. The molecular weight of the PMMA (which is synthesized using the ATRP method) is enhanced with respect to our previous study and the average molecular weight of the PMMA synthesized reached around 270.000 g/mol [~~54~~]. In addition, the increase of the amount of graphene in the PMMA results in an increase of the molecular weight [55]. The improvement in crystallinity with the addition of graphene enhances the mechanical performance of polymer nanocomposites [58-60]. The details regarding the enhancement of the mechanical properties of the polymer nanocomposite have provided some insight into their relationship to their structural properties in this study.

The results have indicated a potential future application for protection of space vehicles from mechanical damage. The mechanical enhancement has allowed practical examination of properties and the crucial benefit for this application of a reduced vehicle mass, which is

critical for aerospace applications. Furthermore, this modified PMMA/GNP nanocomposite has further potential applications in harsh mechanical environments. It was assumed that the specifics of the modified PMMA/GNP nanocomposite were suitable to use in harsh mechanical environments such as in medicinal implants (in joints). Moreover, there is compatibility with IoNT systems to transport medicines to unhealthy parts of the body (even at the cellular level) by using polymer nanocomposites including graphene [61]. This improvement in mechanical properties has offered a potential solution for the need to improve particular properties (e.g. strength and cost) for the ideal selection of materials with synthetic structures. This polymer nanocomposite presents an opportunity for use in load-bearing applications as it has demonstrated a substantial increase in mechanical strength. One area of proposed future work is to extend the use of acoustic signals for monitoring and analysis by applying more advanced acoustic detection and processing techniques used elsewhere [62-63], in order to investigate potential failure mechanisms. It is anticipated that the insight gained by a greater understanding of these failure mechanisms can inform future production of nanocomposites with yet further improved mechanical properties.

4. Conclusions

The addition of a range of concentrations of GNPs to PMMA has provided reinforcement to avoid deformation and mechanical failure in a polymer nanocomposite. The use of ultrasound testing has helped to determine elastic parameters for mechanical modification in the PMMA/GNP nanocomposite synthesized by the “in situ polymerization method” and has been used as an effective method to obtain a suitable modification of this thermoplastic engineering material. The GNPs, at a concentration level of 2 wt.%, were effective in dispersing uniformly in PMMA for the production of a nanocomposite with a defect-free structure as determined by NDT. The addition of GNPs as a nanofiller has changed the mechanical behaviour of the nanocomposite, and in particular a GNP concentration of 2 wt. % increased the compressive strength and hardness of the PMMA/GNP nanocomposite, whilst also reducing the brittleness. NDT test results have been used to support the determination of reliable, rapid and affordable alternative production parameters for the PMMA/GNP nanocomposite. This work, importantly, has also demonstrated that this technique can substantially extend the doping range of GNPs beyond the 1%wt concentrations achieved by previous workers without the consequent deterioration in mechanical properties, but rather with a continuing improvement that follows the trend from lower concentrations. The NDT results have shown that the process used results in a defect-free nanocomposite, as well as

providing a method for nondestructive measurement of these mechanical properties. The results of this study indicate that the improvement in mechanical properties through the production of a homogeneous PMMA/GNP nanocomposite can offer improved possibilities for the deployment of this material in advanced applications compatible with IoNT systems in the near future.

Acknowledgements

This study has been supported by ITU BAP project number 41576, as well as Tubitak in facilitating this collaboration. The synthesis of the nanocomposite was performed in ITU Prof. Dr. Adnan Tekin of the Materials Science & Production Technologies Applied Research Center (ATARC), Istanbul, Turkey. The authors would like to thank Assoc. Prof. Dr. Sinasi EKINCI for his kind assistance with the ultrasound tests at the Nuclear Techniques Department in the Turkish Atomic Energy Authority, Cekmece Nuclear Research and Training Center, Istanbul, Turkey.

References

[1] **W. S. Khan, N. N. Hamadneh, W. A. Khan.** Polymer nanocomposites–synthesis techniques, classification and properties, Science and Applications of Tailored Nanostructures, One Central Press, USA, 2017.

[2] **J. R. Potts, D. R. Dreyer, C. W. Bielawski, R. S. Ruoff.** Graphene-based polymer nanocomposites, *Polym.*, **52**, (2011). 5-25.

[3] **K. I. Winey, R. A. Vaia.** *Polym.* Nanocomposites, *MRS Bulletin*, **32**, (2007). 314-322.

[4] **P. Shapira, J. Youtie, S. Arora.** Early patterns of commercial activity in graphene, *J.of Nanoparticle Res.*, **14**, (2012). 811.

[5] **A. Kausar,** Poly(methyl methacrylate) nanocomposite reinforced with graphene, graphene oxide, and graphite: a review, Polymer-Plastics Technology and Materials 58, 8, (2019) 821–842.

[6] **L. Azevedo, J. L. Antonaya-Martin, P. Molinero-Mourelle, J. del Río-Highsmith,** Improving PMMA resin using graphene oxide for a definitive prosthodontic rehabilitation - A clinical report, J Clin Exp Dent. 11(7) (2019)e670-4.

[7] **Chen G, Weng W, Wu D, Wu C.** PMMA/graphite nanosheets composite and its conducting properties. Eur Polym J 39, 12 (2003) 2329–35.

[8] **B. Li, W.-H. Zhong.** Review on polymer/graphite nanoplatelet nanocomposites, Journal of Materials Science, **46**, (2011) 5595-5614.

[9] **R S Chen, M F H M Ruf, D Shahdan, S Ahmad,** Enhanced mechanical and thermal properties of electrically conductive TPNR/GNP nanocomposites assisted with ultrasonication, PLOS ONE, https://doi.org/10.1371/journal.pone.0222662 (open access), 2019

[10] **J. Ervin, M. Mariatti, S. Hamdan,** Effect of Filler Loading on the Tensile Properties of Multi-walled Carbon Nanotube and Graphene Nanopowder filled Epoxy Composites, Procedia Chemistry, 19 (2016) 897–905.

[11]https://www.nasa.gov/mission_pages/station/research/experiments/explorer/Investigation.html?#id=8071

[12] **Siu-MingYuen, Chen-Chi M.Ma, Chin-Lung Chiang, Jen-An Chang, Sung-Wei Huang, Shia-Chung Chen, Chia-Yi Chuang, Cheng-Chien Yang, Ming-Hsiung Wei,** Silane-modified MWCNT/PMMA composites – Preparation, electrical resistivity, thermal conductivity and thermal stability, Composites Part A: Applied Science and Manufacturing, 38, 12, (2007) 2527-2535.

[13] **L. Y. Zhang, Y. F. Zhang.** In situ fast polymerization of graphene nanosheets-filled poly (methyl methacrylate) nanocomposites, Journal of Applied Polymer Science, (2016) 133.

[14] **J. Wang, H. Hu, X. Wang, C. Xu, M. Zhang, X. Shang.** Preparation and mechanical and electrical properties of graphene nanosheets–poly (methyl methacrylate) nanocomposites via in situ suspension polymerization, Journal of Applied Polymer Science, **122**, (2011). 1866-1871.

[15] **Goncalves, Gil,. P. A. A. P. Marques, A. B.Timmons, I. Bdkin, M. K. Singh, N. Emami and J. Grácioa,** "Graphene oxide modified with PMMA via ATRP as a reinforcement filler." Journal of Materials Chemistry **20.44** (2010) 9927-9934.

[16] **G. Goncalves, S. M. A. Cruz, A. Ramalho, J. Gracio, P.A. Marques,** Graphene oxide versus functionalized carbon nanotubes as a reinforcing agent in a PMMA/HA bone cement, Nanoscale, 2012, 4, 2937-2945.

[17] **P. Kanti D. Pramanık, A. Solanki, A. Debnath, A.Nayyar, S. El-Sappagh, K-S Kwak,** Advancing Modern Health care with Nanotechnology, Nanobiosensors, and Internet of Nano Things: Taxonomies, Applications, Architecture, and Challenges, IEEE Access, 2020, 2984269, 8, pp. 65230-65266.

[18] **R. Sengupta, M. Bhattacharya, S. Bandyopadhyay, A. K. Bhowmick.** A review on the mechanical and electrical properties of graphite and modified graphite reinforced polymer composites, Progress in polymer science, **36**, (2011) 638-670.

[19] **F. A. Settle.** *Handbook of Instrumental Techniques for Analytical Chemistry*, Prentice Hall PTR, (1997).

[20] **J. Blitz, G. Simpson** *Ultrasonic Methods of Non-destructive Test.*, Springer Netherlands, (1995).

[21] **P. Burrascano, S. Callegari, A. Montisci, M. Ricci, M. Versaci.** *Ultrasonic Nondestructive Evaluation Systems: Industrial Application Issues*, Springer International Publishing, (2014).

[22] **D. Royer, D. P. Morgan, E. Dieulesaint.** *Elastic Waves in Solids I: Free and Guided Propagation*, Springer Berlin Heidelberg, (1999).

[23] **A. S. Vasudeva.** *mod. Engneering phys.*, S. Chand Limited, (2012).

[24] **H. Chandler, A. International.** *Hardness Testing, 2nd Edition*, ASM International, (1999).

[25] **L. Y. Zhang, Y. F. Zhang.** In situ fast polymerization of graphene nanosheets-filled poly (methyl methacrylate) nanocomposites, *J. of appl. Polym. Science*, **133** (2016).

[26] **X. Wang, J. Li, W. Qu, G. Chen.** Fabrication of graphene/poly(methyl methacrylate) composite electrode for capillary electrophoretic determination of bioactive constituents in Herba Geranii, *J. of Chromatography A*, **1218**, (2011) 5542-5548.

[27] **B. H. Stuart.** *Infrared Spectroscopy: Fundamentals and Applications*, Wiley, (2004).

[28] **M. Reyes-Acosta, A. Torres-Huerta, M. Domínguez-Crespo, A. Flores-Vela, H. Dorantes-Rosales, J. Andraca-Adame.** Thermal, Mechanical and UV-Shielding Properties of Poly(Methyl Methacrylate)/Cerium Dioxide Hybrid Systems Obtained by Melt Compounding, *Polym.*, **7**, (2015) 1474.

[29] **M. Ara, K. Wadumesthrige, T. Meng, S. O. Salley, K. S. Ng.** Effect of microstructure and Sn/C ratio in SnO 2–graphene nanocomposites for lithium-ion battery performance, *Rsc Advances*, **4**, (2014) 20540-20547.

[30] **E. Naveau.** Preparation of new organoclays in supercritical carbon dioxide and their industrial potential in polymer nanocomposites, Faculty of Sciences Center for Education and Research on Macromolecules, CERM, Doctorate Thesis, (2012).

[31] **B. W. Chieng, N. A. Ibrahim, W. M. Z. Wan Yunus, M. Z. Hussein, V. S. G. Silverajah.** Graphene Nanoplatelets as Novel Reinforcement Filler in Poly(lactic acid)/Epoxidized Palm Oil Green Nanocomposites: Mechanical Properties, *International J. of Molecular Sciences*, **13**, (2012) 10920.

[32] **Z. Z. Wang, S. H. Xu, L. X. Wu, D. X. Zhuo,** Advanced Materials Research, Trans Tech Publ, (2014) 31-34.

[33] **X. Yuan, L. Zou, C. Liao, J. Dai.** Improved properties of chemically modified graphene/poly (methyl methacrylate) nanocomposites via a facile in-situ bulk polymerization, *Expr.Polym. Letters*, **6**, (2012) 847-858.

[34] **Y.-K. Yang, C.-E. He, R.-G. Peng, A. Baji, X.-S. Du, Y.-L. Huang, X.-L. Xie, Y.-W. Mai.** Non-covalently modified graphene sheets by imidazolium ionic liquids for multifunctional polymer nanocomposites, *J. of Materials Chemistry*, **22**, (2012) 5666-5675.

[35] **V. Poblete, M. Alvarez, V. Fuenzalida.** Conductive copper-PMMA nanocomposites: Microstructure, electrical behavior, and percolation threshold as a function of metal filler concentration, *Polym. Composites*, **30**, (2009) 328-333.

[36] **H. Pang, T. Chen, G. Zhang, B. Zeng, Z.-M. Li.** An electrically conducting polymer/graphene composite with a very low percolation threshold, *Mater. Letters*, **64**, (2010) 2226-2229.

[37] **T. Ramanathan, S. Stankovich, D. Dikin, H. Liu, H. Shen, S. Nguyen, L. Brinson.** Graphitic nanofillers in PMMA nanocomposites—an investigation of particle size and dispersion and their

influence on nanocomposite properties, *J. of Polym. Science Part B: Polym. phys.,* **45**, (2007) 2097-2112.

[38] **G. Chen, W. Weng, D. Wu, C. Wu.** PMMA/graphite nanosheets composite and its conducting properties, *European Polymer Journal*, **39**, (2003) 2329-2335.

[39] **H. A. Afifi.** Ultrasonic pulse echo studies of the physical properties of PMMA, PS, and PVC, *Polym.-Plastics Technology and Engineering*, **42**, (2003) 193-205.

[40] **B. Das, K. E. Prasad, U. Ramamurty, C. Rao.** Nano-indentation studies on polymer matrix composites reinforced by few-layer graphene, *nanotechnol.*, **20**, (2009) 125705.

[41] **T. M. Al-Saadi, M. A. Jihad.** Preparation and Characterization of Graphene/PMMA Composite, International J. of Advanced Res. in Science, Engineering and Technology, 2, 10, (2015).

[42] **D. Galpaya, M. Wang, M. Liu, N. Motta, E. Waclawik, C. Yan.** Recent advances in fabrication and characterization of graphene-polymer nanocomposites, Graphene, 1, (2012). 30-49

[43] **J. Wang, H. Hu, X. Wang, C. Xu, M. Zhang, X. Shang.** Preparation and mechanical and electrical properties of graphene nanosheets–poly (methyl methacrylate) nanocomposites via in situ suspension polymerization, *J. of appl. Polym. Science*, **122**, (2011) 1866-1871.

[44] Ryu, S. H., Kim, S., Kwon, Y. T., Park, Y. K., Kang, S. O., Cho, H. B., & Choa, Y. H. (2020). Decorating surface charge of graphite nanoplate using an electrostatic coupling agent for 3- dimensional polymer nanocomposite. Journal of Applied Polymer Science, 137(8), 48390.

[45] Mutlay, İ., & Tudoran, L. B. (2014). Percolation behavior of electrically conductive graphene nanoplatelets/polymer nanocomposites: theory and experiment. Fullerenes, Nanotubes and Carbon Nanostructures, 22(5), 413-433.

[46] **T. Bel, C. Arslan, N. Baydogan.** Radiation shielding properties of poly (methyl methacrylate)/colemanite composite for the use in mixed irradiation fields of neutrons and gamma rays, *Materials Chemistry and Physics*, **221,** (2019) 58-67.

[47] **J.Cuthbert, S. S. Yerneni, M. Sun, T. Fu, and Krzysztof Matyjaszewski,** Degradable Polymer Stars Based on Tannic Acid Cores by ATRP, Polymers, 11, 5 (2019) 752.

[48] **N. You, C. Zhang, Y. Liang, Q. Z. P. Fu, M. Liu, Q. Zhao, Z. Cui, X. Pang,** Facile Fabrication of SizeTunable Core/Shell Ferroelectric/ Polymeric Nanoparticles with Tailorable Dielectric Properties via Organocatalyzed Atom Transfer Radical Polymerization Driven by Visible Light, Scientific Reports, 9 (2019) 1869

[49] **C.N. Yan, Q. Liu, L. Xu, L.P Bai, L.Pi. Wang, G. Li,** Photoinduced Metal-Free Surface Initiated ATRP from Hollow Spheres Surface, Polymers 11 (2019) 599

[50] **F. J. Tommasini, L. C. Ferreira, L. G. P. Tienne, V. O. Aguiar, M. H. P. Silva, L. F. M. Rocha, M.F.V. Marques,** Poly (Methyl Methacrylate)-SiC Nanocomposites Prepared Through in Situ Polymerization, Materials Research. 21, 6 (2018) e20180086

[51] **D. Sethy, S. Makireddi, F. V. Varghese, K. Balasubramaniam,** Piezoresistive behaviour of graphene nanoplatelet GNP/PMMA spray coated sensors on a polymer matrix composite beam, eXPRESS Polymer Letters, 13, 11 (2019) 1018–1025

[52] **B. Alemour, O. Badran, M. R. Hassan,** A Review of Using Conductive Composite Materials in Solving Lightening Strike and Ice Accumulation Problems in Aviation, J. Aerosp. Technol. Manag., São José dos Campos, 11, (2019), e1919,

[53] https://iss.jaxa.jp/en/kuoa/news/seuwg_26th.html

[54] https://iss.jaxa.jp/en/kuoa/images/APRSAF-26%20Reports_SEUWG.pdf

[55]https://www.nasa.gov/mission_pages/station/research/experiments/explorer/Investigation.html?#id=8071

[56] Y. Yigit, A. Kilislioglu, S. Karakus, N. Baydogan, Determination of the intrinsic viscosity and molecular weight of Poly(methyl methacrylate) blends, Journal of Investigations on Engineering and Technology, Vol. 2, Iss. 2, 2019, ISSN: 2687-3052

[57] Hui Wang, Letian Wang, Shanyu Meng, Hanxue Lin, Melanie Correll and Zhaohui Tong, Nanocomposite of Graphene Oxide Encapsulated in Polymethylmethacrylate (PMMA): Pre-Modification, Synthesis, and Latex Stability, J. Compos. Sci. 2020, 4, 118; doi:10.3390/jcs4030118

[58] J. Zhu, H. Zhang, N. A. Kotov, Thermodynamic and Structural Insights into Nanocomposites Engineering by Comparing Two Materials Assembly Techniques for Graphene, ACS Nano, Vol. 7, No. 6, 4818–4829, 2013, doi.org/10.1021/nn400972t

[59] E. Ahn, T. Lee, M. Gu, M. Park, S. H. Min, B-Su Kim, Layer-by-Layer Assembly for Graphene-Based Multilayer Nanocomposites: The Field Manual, Chem. Mater. 2017, 29, 1, 69–79 doi.org/10.1021/acs.chemmater.6b02688

[60] N. A. Kotov, I. Dekdny, J. H. Fendler, Layer-by-Layer Self-Assembly of Polyelectrolyte-Semiconductor Nanoparticle Composite Films, J. Phys. Chem. 1995, 99, 13065-13069, doi.org/10.1021/j100035a005

[61] P. Kanti Dutta Pramanik, A. Solank , A. Debnath, A.d Nayyar, S. El-Sappagh, Kyung-Sup Kwak, Advancing Modern Healthcare with Nanotechnology, Nanobiosensors, and Internet of Nano Things: Taxonomies, Applications, Architecture, and Challenges, IEEE Acess, Vol. 8, 65230-65266.

[62] **L. Yao, P. Lv, G. Bai, X. Tong, and A. T. Augousti,** Influence of Low Velocity Impact on Oxidation Performance of SiC coated C/SiC Composites *Ceramics International* **45(**16) p20470-7 https://doi.org/10.1016/j.ceramint.2019.07.025

[63] **P. Lyu, L. Yao, G. An, G. Bai, and A. T. Augousti,** Correlation between failure mechanism and rupture lifetime of 2D-C/SiC under stress oxidation conditions based on acoustic emission pattern recognition *Journal of the European Ceramics Society* DOI: 10.1016/j.jeurceramsoc.2020.06.070. 29 June 2020

Figure Captions

Figure 1: A schematic diagram displaying the steps in the polymerization process used to make the PMMA/GNPs nanocomposite.

Figure 2. FTIR spectra of Pure PMMA and PMMA /GNPs nanocomposites.

Figure 3. XRD patterns of PMMA, GNPs and PMMA/GNPs nanocomposites.

Figure 4. Rockwell hardness values of PMMA/GNPs nanocomposites.

Figure 5. The images of PMMA/GNPs nanocomposite samples after the compression test.

Figure 6. The changes in compressive strength of PMMA/GNPs nanocomposites.

Figure 7. Raman spectra of the PMMA/GNPs nanocomposite samples.

Table Captions

Table 1: The changes in elastic parameters of PMMA/GNPs.

Table 2. Comparison of physical properties of PMMA/GNPs nanocomposite samples produced by the ATRP method in this study and in the literature.

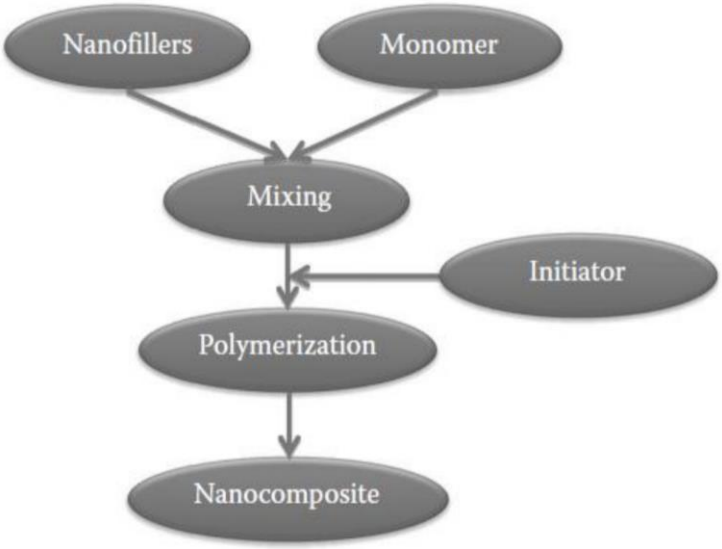
Nanofillers
Monomer
Mixing
Initiator
Polymerization
Nanocomposite

Figure 1.

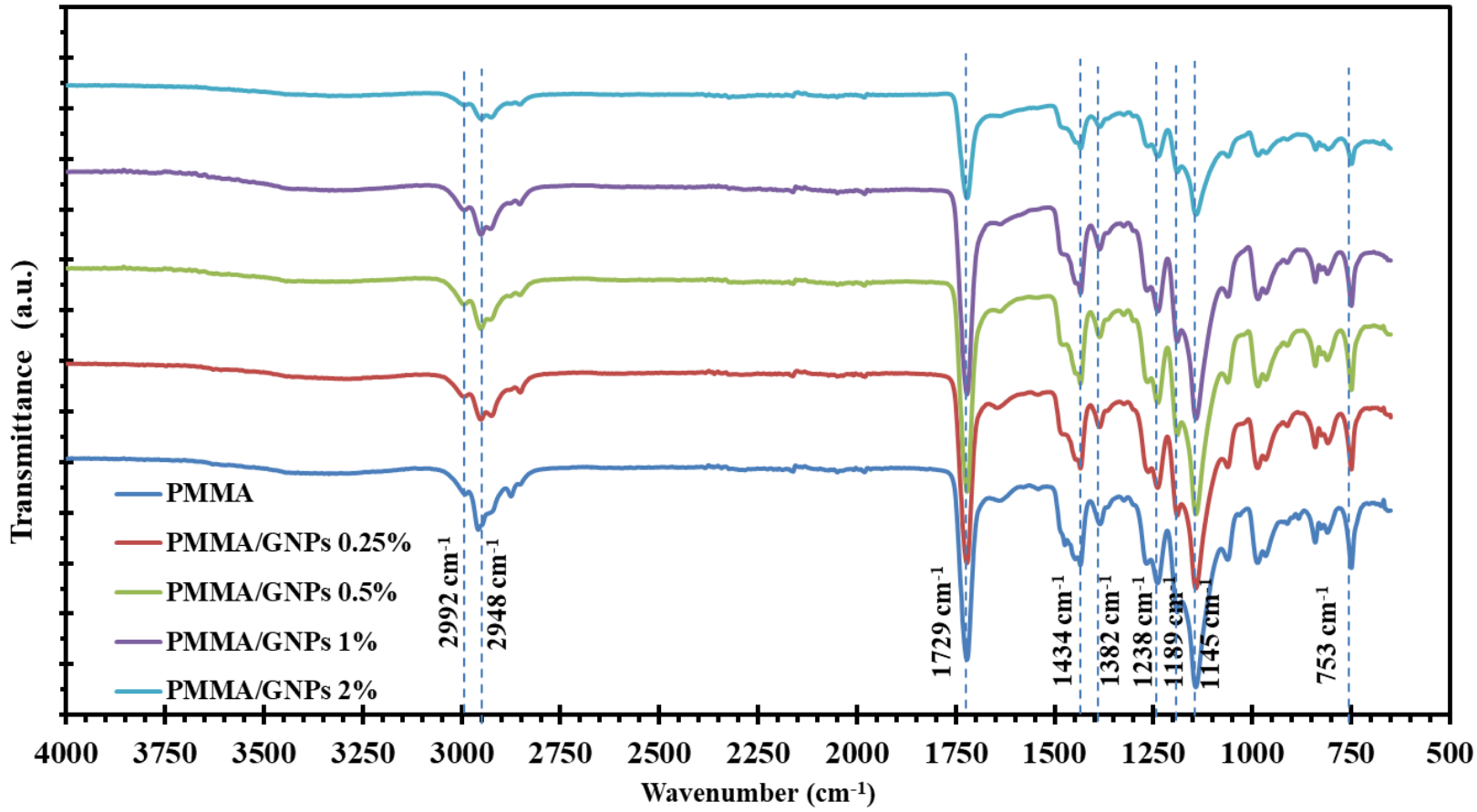
Transmittance (a.u.)
PMMA
PMMA/GNPs 0.25%
PMMA/GNPs 0.5%
PMMA/GNPs 1%
PMMA/GNPs 2%
2992 cm-1
2948 cm-1
1729 cm-1
1434 cm-1
1382 cm-1
1238 cm-1
1189 cm-1
1145 cm-1
753 cm-1
4000 3750 3500 3250 3000 2750 2500 2250 2000 1750 1500 1250 1000 750 500
Wavenumber (cm-1)

Figure 2.

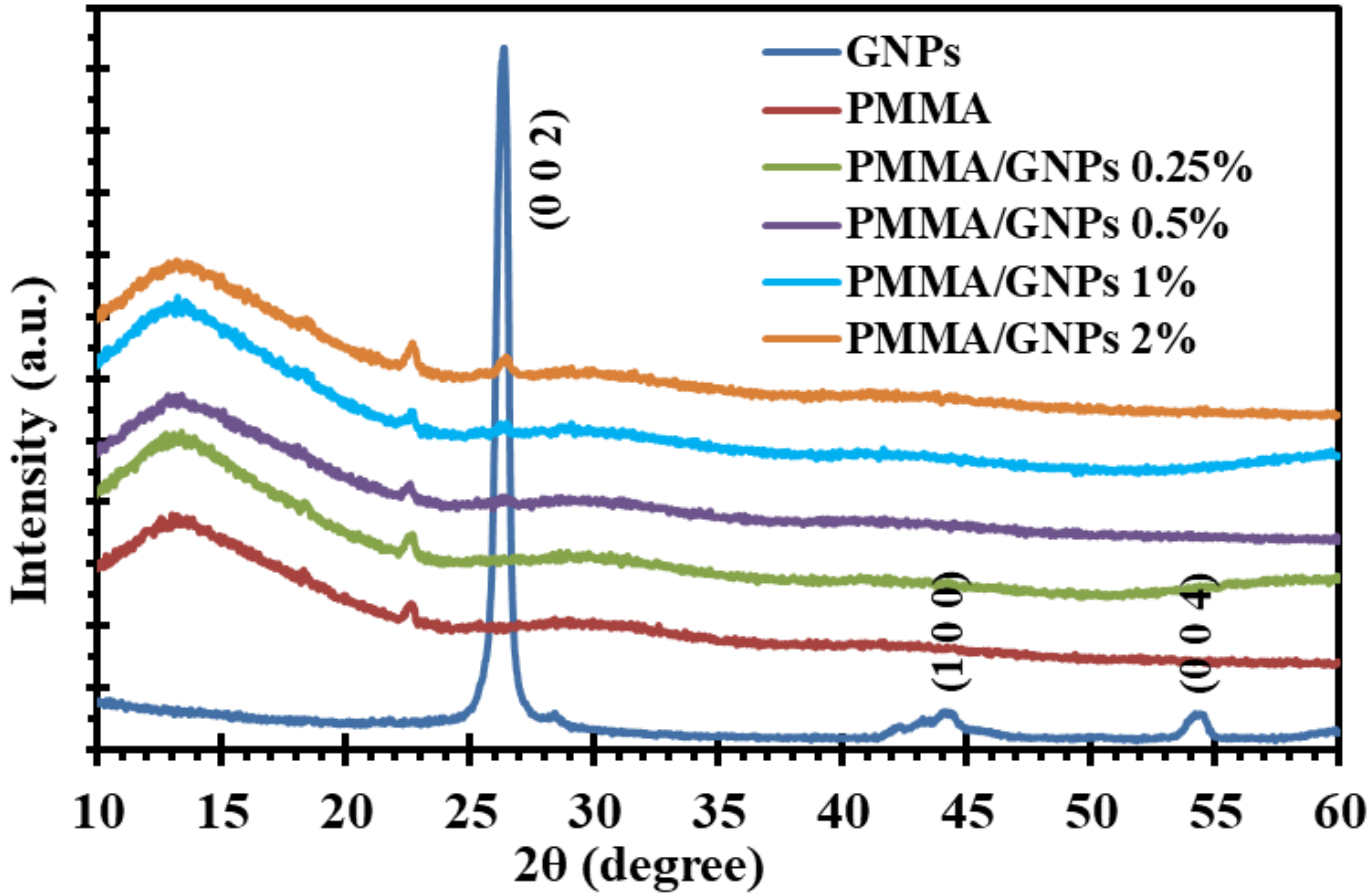
GNPs
PMMA
PMMA/GNPs 0.25%
PMMA/GNPs 0.5%
PMMA/GNPs 1%
PMMA/GNPs 2%
(0 0 2)
(1 0 0)
(0 0 4)
Intensity (a.u.)
10
15
20
25
30
35
40
45
50
55
60
2θ (degree)

Figure 3.

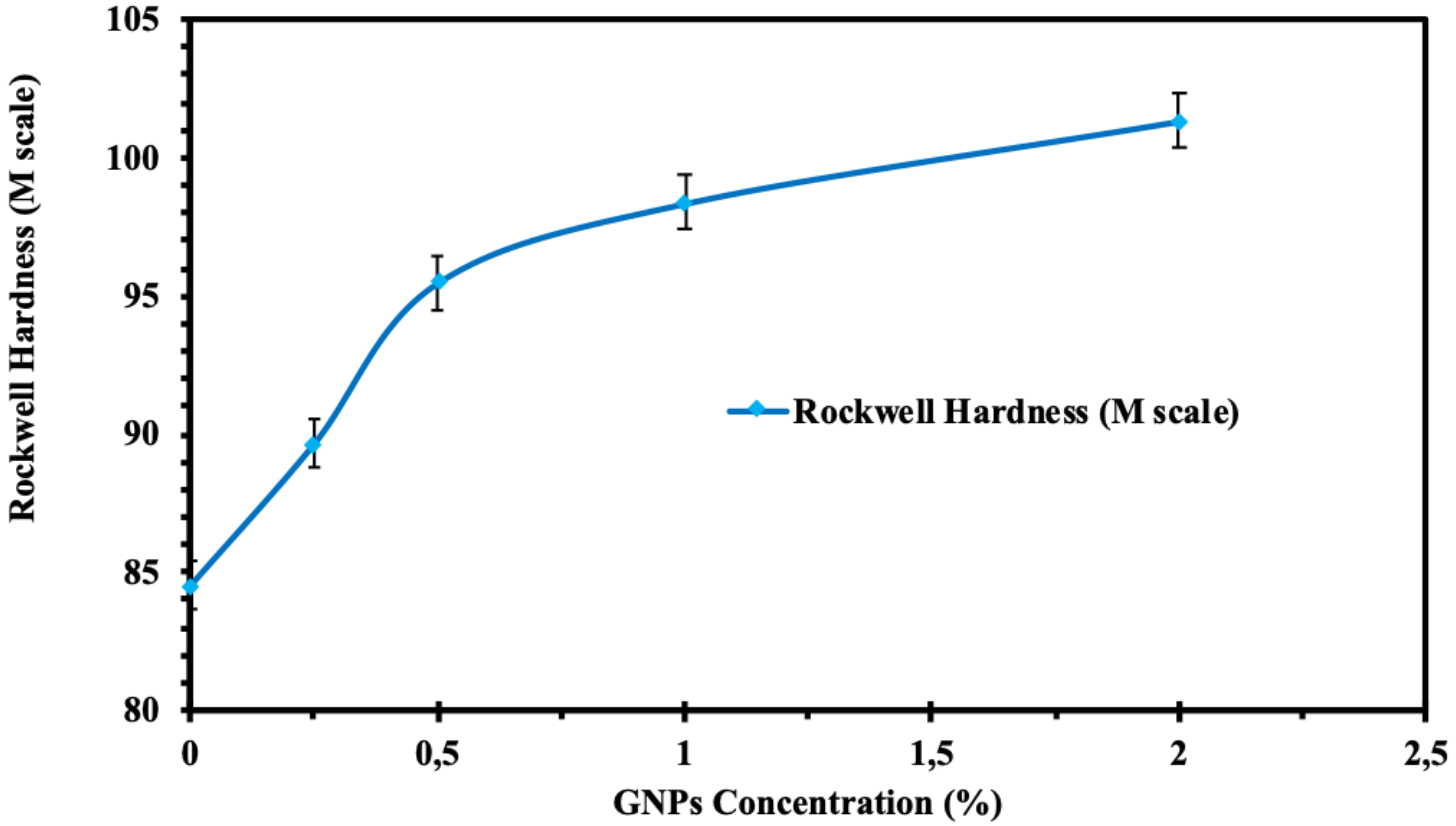
105
100
95
90
85
80
Rockwell Hardness (M scale)
0
0,5
1
1,5
2
2,5
GNPs Concentration (%)
Rockwell Hardness (M scale)

Figure 4.

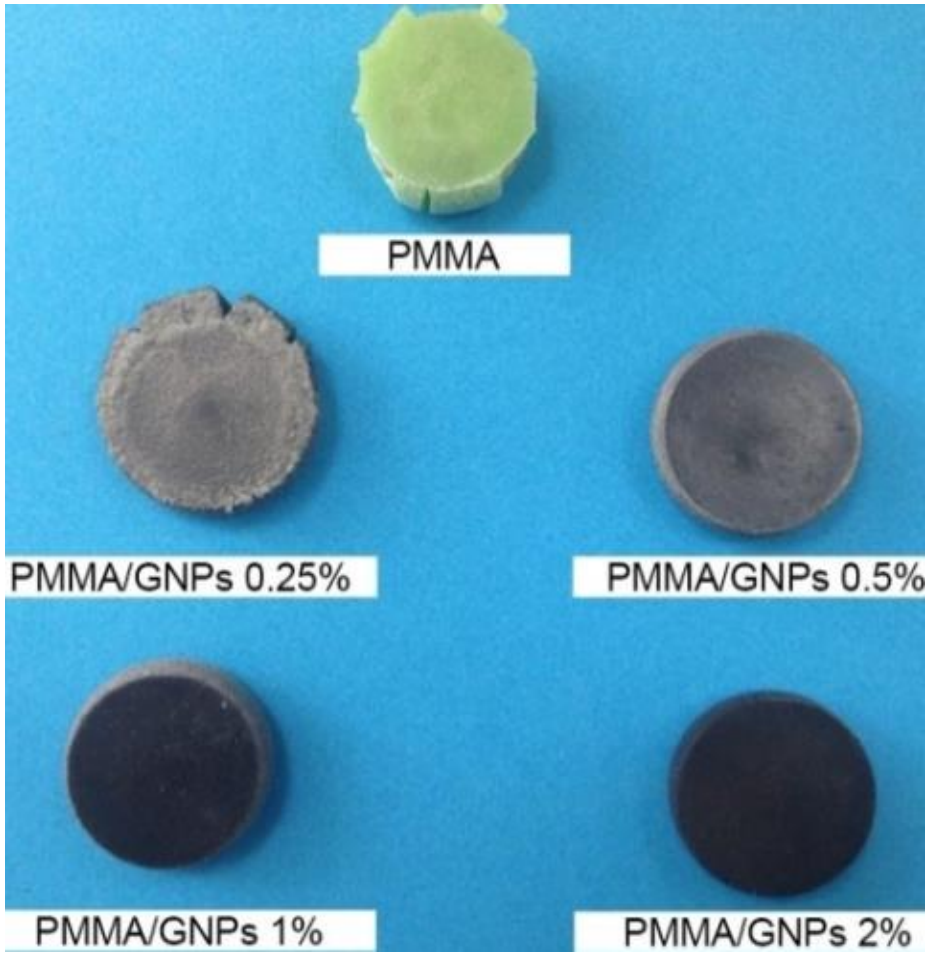

(a)

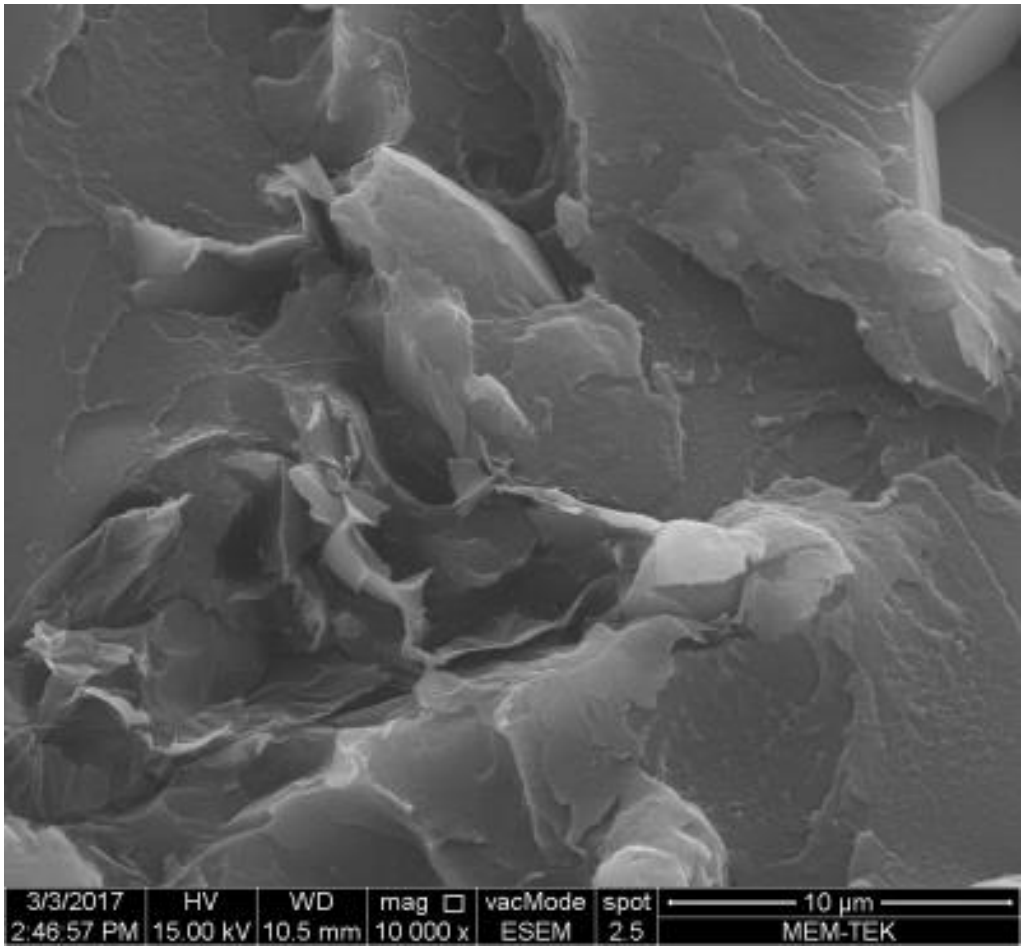

(b)

Figure 5(a-b).

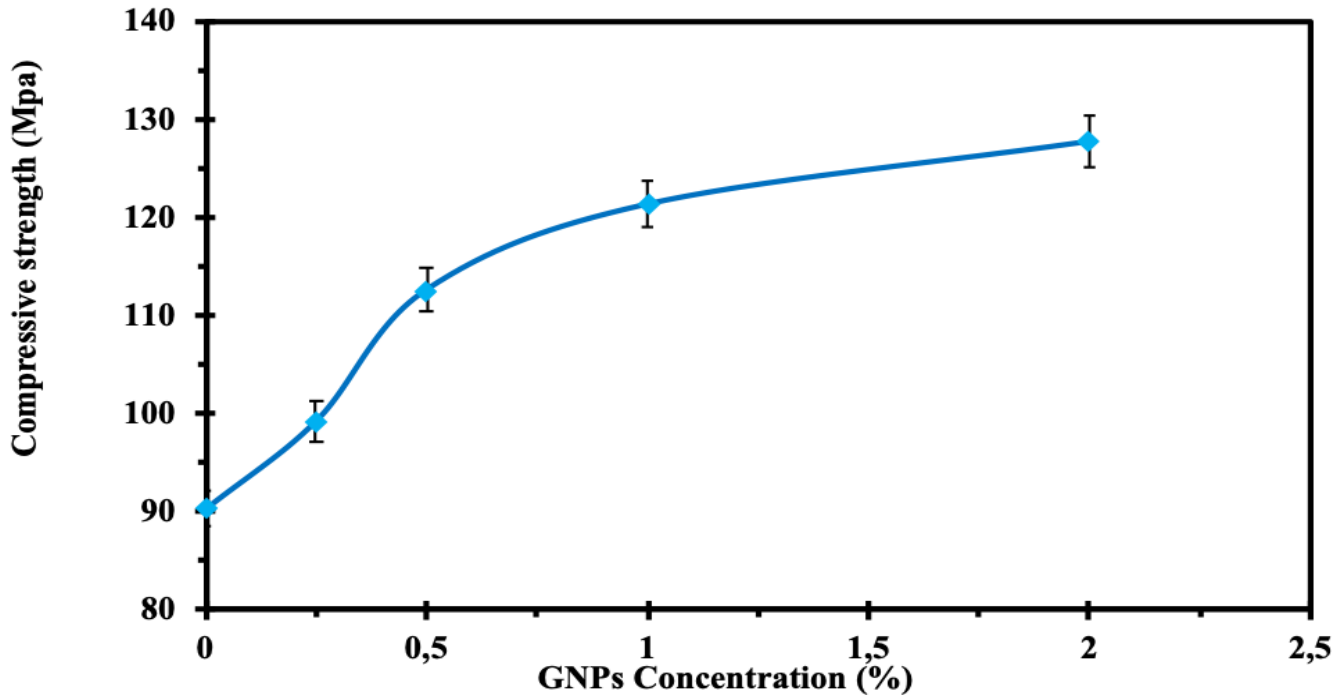
Compressive strength (Mpa)
140
130
120
110
100
90
80
0
0,5
1
1,5
2
2,5
GNPs Concentration (%)

Figure 6.

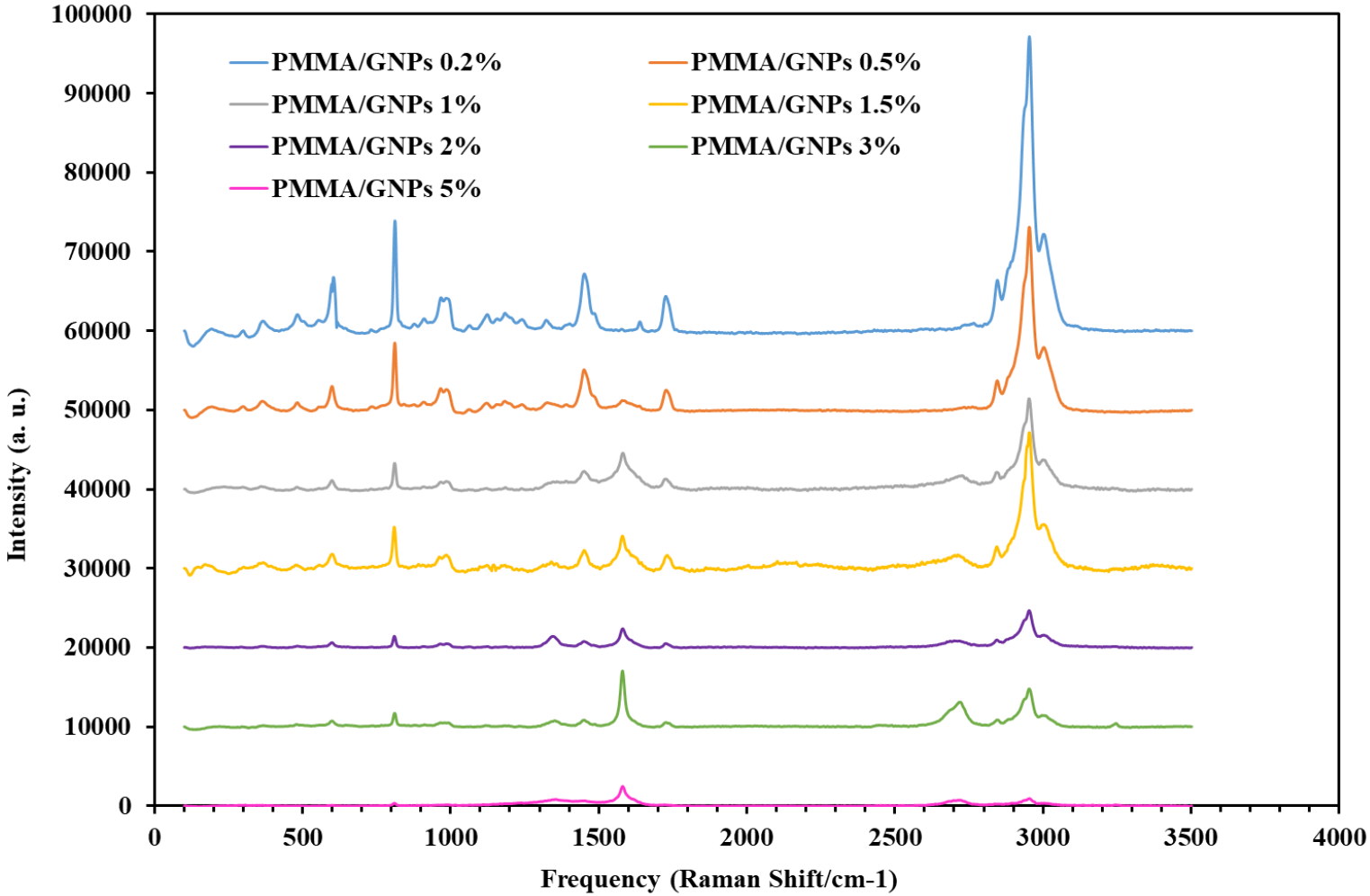
PMMA/GNPs 0.2%
PMMA/GNPs 0.5%
PMMA/GNPs 1%
PMMA/GNPs 1.5%
PMMA/GNPs 2%
PMMA/GNPs 3%
PMMA/GNPs 5%
Intensity (a. u.)
Frequency (Raman Shift/cm-1)
100000
90000
80000
70000
60000
50000
40000
30000
20000
10000
0
0
500
1000
1500
2000
2500
3000
3500
4000

Figure 7.

Table 1: The changes in elastic parameters of PMMA/GNPs.

GNPs Concent. in PMMA (wt. %)	ρ Density (kg/m^3)	C_L Longitudinal velocity (m/s)	C_T Transverse velocity (m/s)	ν Poisson's ratio	G Shear modulus (Gpa)	E Young's modulus (Gpa)	H Microhardness (Gpa)
0.00	1180.890	2663.508	1322.011	0.337	2.064	5.517	0.225
0.25	1184.130	2699.876	1338.528	0.337	2.122	5.673	0.230
0.50	1187.920	2736.923	1356.172	0.337	2.185	5.843	0.237
1.00	1193.180	2786.545	1377.294	0.338	2.263	6.058	0.244
2.00	1204.110	2863.278	1414.000	0.339	2.407	6.446	0.259

Table 2. Comparison of the physical properties of PMMA/GNPs nanocomposite samples produced by the ATRP method in this study and in the literature**.**

Researchers	Applied method	Thermal properties	Changes in mechanical properties
Gil et al. [15]	Solution mixing	The temperature at 10% weight loss was improved ~ 50°C at 2 wt. % by using graphene oxide	• Elastic modulus improved ~ 16 % • Tensile strength improved ~18 % at 1 wt. % , higher concentration of GNPs resulted in a deterioration of the mechanical properties.
Zhang et al. [13]	In situ fast polymerization	5% weight loss temperature increased ~ 41 °C at 2 wt. % by using graphene nanosheets	• Elastic modulus improved ~ 14% , • Rockwell Hardness (C scale) improved ~5% • Tensile strength improved ~41% compare to pure PMMA at 0.3 wt. % GNP concentration, higher GNPs concentration resulted in a deterioration of the mechanical properties.
Wang et al. [14]	In situ polymerization	5% weight loss temperature increased ~ 40 °C at 1 wt. % by using graphene nanosheets	• Tensile strength ~ 60 % at 1 wt. % higher GNPs concentration resulted in a deterioration of the mechanical properties .
This study	In situ ATRP polymerization	5% weight loss temperature increased by ~ 46 °C at 2 wt. %	• Elastic modulus improved ~16.8 %, • Rockwell hardness (M scale) improved ~ 19.9% • Microhardness improved ~ 14.2%, • Shear modulus improved ~ 19.5%, • Compressive strength improved ~ 42.7% compared to pure PMMA at 2 wt.% GNP concentration. • Tensile strength test (as the maximum stress) was not conducted in the same sample mold (which was used for other mechanical tests in this study).Tensile strength tests (for maximum stress achievable) were not able to be conducted in the same sample mould (which was used for other mechanical tests in this study).